Thermal collapse of a granular gas under gravity

Dmitri Volfson,[1,2] Baruch Meerson,[3] and Lev S. Tsimring[2]
[1]*Bioengineering Department, University of California, San Diego, La Jolla, California 92093-0402, USA*
[2]*Institute for Nonlinear Science, University of California, San Diego, La Jolla, California 92093-0402, USA*
[3]*Racah Institute of Physics, Hebrew University of Jerusalem, Jerusalem 91904, Israel*
(Received 13 December 2005; published 23 June 2006)

Free cooling of a gas of inelastically colliding hard spheres represents a central paradigm of kinetic theory of granular gases. At zero gravity the temperature of a freely cooling *homogeneous* granular gas follows a power law in time. How does gravity, which brings inhomogeneity, affect the cooling? We combine molecular dynamics simulations, a numerical solution of hydrodynamic equations and an analytic theory to show that a granular gas cooling under gravity undergoes thermal collapse: it cools down to zero temperature and condenses on the bottom of the container in a finite time.

DOI: 10.1103/PhysRevE.73.061305 PACS number(s): 45.70.Qj, 47.70.Nd

Granular gas, a low-density fluid of inelastic hard spheres, is a simple model of granular flow, and it has attracted much attention from physicists [1,2]. An undriven granular gas loses its kinetic energy via inelastic collisions. In the homogeneous cooling state (HCS) the temperature T of a dilute granular gas decays according to Haff's law [1], $T(t)=T_0(1+t/t_0)^{-2}$, where in two dimensions $t_0=\sqrt{\pi}/2(1-r^2)dn_0T_0^{1/2}$ is the cooling time, n_0 is the (constant) number density of the particles, d is the particle diameter and r is the coefficient of normal restitution. The HCS, and deviations from it, provide a rich testing ground for the ideas and methods of kinetic theory of granular gases, and it has been investigated in many theoretical works, see Ref. [2] and references therein. Direct experimental observation of the HCS is difficult, not the least because of gravity. Therefore it is somewhat surprising that there have been no theoretical studies of the effect of gravity on the free cooling of a granular gas. It is intuitively clear that gravity forces grains to sink to the bottom of the container, where increased density enhances the collision rate and causes "freezing" of the granulate. However, to our knowledge, no quantitative analysis of this process has ever been performed. Here we combine molecular dynamics (MD) simulations, a numerical solution of granular hydrodynamic equations and analytical theory to develop a detailed quantitative understanding of this cooling process. Our main result is that, in a striking contrast to Haff's law, the gas undergoes thermal collapse: it cools down to zero temperature and condenses on the bottom plate in a finite time exhibiting, close to collapse, a previously unknown universal scaling behavior.

MD simulations. We employed an event-driven algorithm [3] to simulate a free cooling of an initially dilute gas of $N\gg 1$ identical nearly elastic, $1-r\ll 1$, hard disks of unit diameter and mass in a two-dimensional container of width L_x and infinite height. The (elastic) bottom of the container is at $y=0$, the (elastic) sidewalls are at $x=0$ and L_x. L_x is chosen small enough so that any macroscopic structure in the lateral direction is suppressed. The gravity acceleration g acts in the negative y direction. Figure 1 shows four snapshots of a typical simulation where, at $t=0$, particles have a Maxwell velocity distribution, and a Boltzmann density profile at constant temperature T_0 [4]. Collapse of all particles to the bottom is observed at time $t_c=7770$. The circles in Fig. 2(a) show the time history of the simulated total kinetic energy of the gas, normalized to its value at $t=0$. One can see that the total energy drops to zero in a finite time. We observed a similar behavior in a wide range of parameters, and also for a different, *nonisothermal* initial state, prepared by replacing the elastic bottom plate by a "thermal" bottom plate [3] and waiting until a steady state is reached. In the latter case the initial transient is somewhat different, but the energy decay law close to collapse remains the same, see Fig. 2(a).

Hydrodynamic theory. The observed energy decay dynamics are remarkably captured by hydrodynamic equations for the number density $n(y,t)$, vertical velocity $v(y,t)$ and granular temperature $T(y,t)$. These equations are systematically derivable from the Boltzmann equation generalized to account for inelastic collisions of hard disks [2,5]. We assume a dilute gas, an assumption which becomes invalid close to collapse [6]. Following Ref. [7], we rescale the variables using the gravity length scale $\lambda=T_0/g$ and the heat diffusion time $t_d=\varepsilon^{-1}(\lambda/g)^{1/2}$. The scaled parameter $\varepsilon=\pi^{-1/2}(L_x/Nd)\ll 1$ is of the order of the inverse number of layers of grains which form after the particles settle on the bottom. The smallness of ε guarantees that t_d is much longer than the fast hydrodynamic time $t_f=(\lambda/g)^{1/2}$. We measure v in units of $v_0=\lambda/t_d$, n in units of $n_0=N/\lambda L_x$, and T in units of T_0. Furthermore, we exploit the one dimensionality of the flow and go over to Lagrangian mass coordinate $m=\int_0^y n(y',t)dy'$ which varies between 0 at

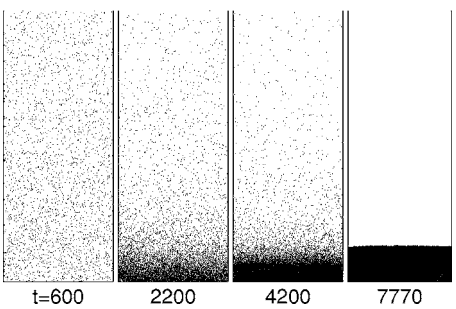

FIG. 1. Snapshots of an event-driven MD simulation at indicated times for $N=5642$, $L_x=10^2$, $r=0.995$, $T_0=10$ and $g=0.01$. Only a part of the box in the lateral direction is shown.

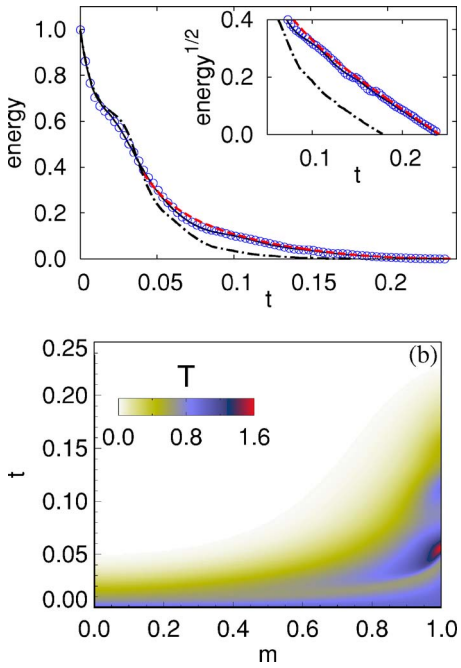

FIG. 2. (Color online) (a) Total kinetic energy of the grains, normalized to its value at $t=0$, vs time for the run in Fig. 1 (circles). Also shown are the results from the full hydrodynamic model (1)–(3) (black solid line), from Eq. (4) (red dashed line), and from a MD simulation with a *different*, nonisothermal initial condition (black dash-dotted line). The respective hydrodynamic parameters are $\varepsilon=10^{-2}$ and $\Lambda=5$. The inset shows the square root of the energy close to thermal collapse. (b) A space-time plot of T from the full hydrodynamic model for the same simulation.

the bottom and 1 (the total rescaled mass of the gas) as $y\to\infty$. The resulting rescaled hydrodynamic equations are [7,8]:

$$\partial_t(1/n) = \partial_m v, \tag{1}$$

$$\varepsilon^2\partial_t v = -\partial_m(nT) - 1 + (\varepsilon^2/2)\partial_m(nT^{1/2}\partial_m v), \tag{2}$$

$$\partial_t T + nT\partial_m v = (\varepsilon^2/2)nT^{1/2}(\partial_m v)^2 + (4/3)\partial_m(n\partial_m T^{3/2}) - 4\Lambda^2 nT^{3/2}. \tag{3}$$

In addition to ε, Eqs. (1)–(3) include the parameter $\Lambda^2=\frac{1-r^2}{4\varepsilon^2}$ which shows the relative role of the inelastic energy loss and heat diffusion. At the boundaries $y=0$ and ∞ we demand zero fluxes of mass, momentum and energy [7], which yield $v=\partial_m T=0$ at $m=0$ and $n\partial_m v=n\partial_m T=0$ at $m=1$.

We solved Eqs. (1)–(3) numerically in a wide range of parameters, using a variable mesh/variable time step solver [9]. The black solid line in Fig. 2(a) depicts the sum of the thermal energy and macroscopic kinetic energy of the gas versus time for the same parameters and initial condition as in the MD simulation indicated by the circles. The agreement is excellent, and thermal collapse is clearly observed [6]. At the very early stage of the cooling [with duration of $\mathcal{O}(\tau_f)$] we observed shock waves which form at large heights, cause a transient heating of the gas there, and escape to $m=1$ ($y=\infty$), see Fig. 2(b).

Quasi-static flow. If $\varepsilon\ll\min(1,\Lambda^{-2})$ then, after the brief transient, a *quasi-static* flow sets in. Here the ε^2 terms in Eqs. (2) and (3) can be neglected, and Eq. (2) reduces to the hydrostatic condition $\partial_m(nT)+1=0$ which yields $nT=1-m$. Substituting $n=(1-m)/T$ into Eq. (3) and using Eq. (1), we obtain a closed nonlinear equation for a new variable $\omega(m,t)=T^{1/2}(m,t)$

$$\omega\partial_t\omega = \partial_m[(1-m)\partial_m\omega] - \Lambda^2(1-m)\omega. \tag{4}$$

We will call Eq. (4) the ω equation; it was derived, in another context, in Ref. [7].

We solved the ω equation numerically [with the no-flux boundary conditions $(1-m)\partial_m\omega=0$ at $m=0$ and 1], using the same solver [9]. A typical example is shown in Fig. 2(a). Here we launched the computation at scaled time $t=0.04$ when the hydrostatic condition $nT=1-m$ already holds well, and used the temperature profile, computed with the full hydrodynamic solver, as the initial condition. One can see that the ω equation provides a faithful description of the later stage of the cooling. Figure 3 shows a different example of the cooling dynamics, as described by the ω equation starting from $\omega(m,t=0)=1$. Here we show the T and v profiles in both Lagrangian and Eulerian coordinates. In all simulations thermal collapse is observed at a time t_c which goes down as Λ increases. The collapse occurs simultaneously on the whole Lagrangian interval $(0,1)$, see Fig. 3(a). As the density $n=(1-m)/T$ blows up at $t=t_c$ at all $m\in[0,1)$, this Lagrangian interval corresponds to a single Eulerian point $y=0$. Therefore, at time $t=t_c$ *all* of the gas condenses on the bottom plate $y=0$ and cools to a zero temperature [10].

Separable solution close to collapse. As Fig. 3(d) implies, $\omega(m,t)$ becomes separable as $t\to t_c$. This remarkable solution can be written as

$$\omega(m,t) = (t_c - t)Q(m), \tag{5}$$

where $Q(m)$ is determined by the nonlinear ordinary differential equation

$$[(1-m)Q']' - \Lambda^2(1-m)Q + Q^2 = 0 \tag{6}$$

(the primes denote m derivatives) and the boundary conditions $(1-m)Q'=0$ at $m=0$ and 1. Function $Q(m)$ is uniquely determined by Λ and, at fixed Λ, can be found numerically by shooting. In addition, we found $Q(m)$ perturbatively for small and large Λ:

I. $\Lambda^2\ll 1$. As it can be checked *a posteriori*, in this case $Q(m)=\mathcal{O}(\Lambda^2)$. Furthermore, as the heat diffusion dominates over the inelastic energy loss, the solution must be almost constant on the whole interval $0\le m<1$. Therefore, we seek a solution in the form $Q(m)=\Lambda^2 Q_0+\Lambda^4 Q_1(m)+\Lambda^6 Q_2(m)+\ldots$. Substituting this in Eq. (6) and equating terms of the same order in Λ^2, we obtain the asymptotic solution

$$Q(m) = \frac{\Lambda^2}{2} - \frac{\Lambda^4}{16} + \frac{\Lambda^4 m^2}{8} + \mathcal{O}(\Lambda^6). \tag{7}$$

We checked that this solution is in excellent agreement with numerical solutions of the ω equation at small Λ.

II. $\Lambda^2\gg 1$. Here it is convenient to stretch the Lagrangian

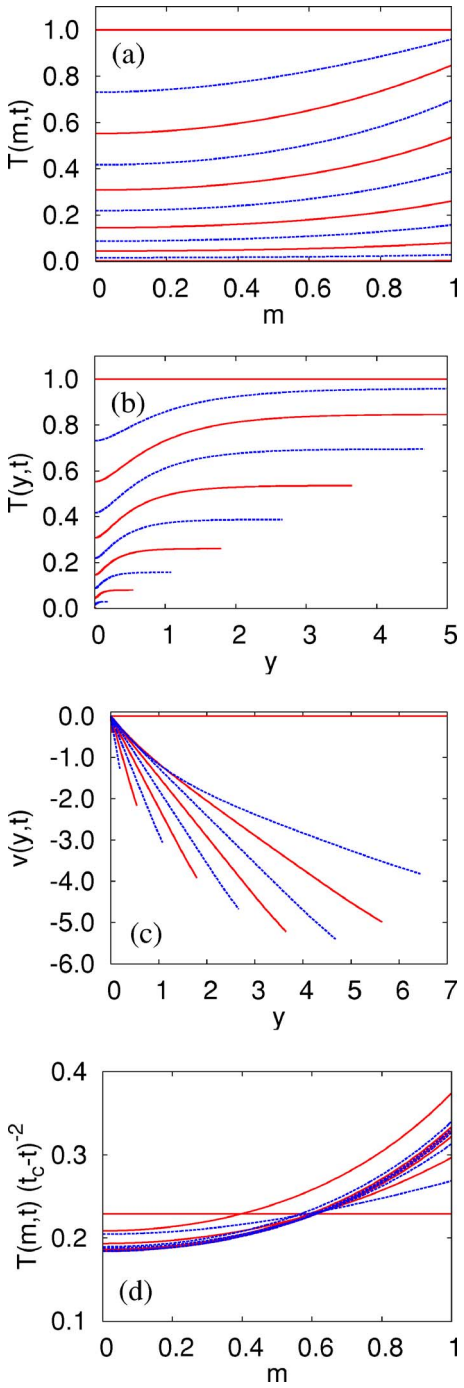

FIG. 3. (Color online) Hydrodynamic fields predicted by the ω equation for $\Lambda=1$: $T(m,t)$ at times separated by $\Delta t=0.2$ (a), and $T(y,t)$ (b), $v(y,t)$ (c), and $T(m,t)(t_c-t)^{-2}$ (d) at the same times. The late-time curves in (d) collapse into a single curve.

coordinate, $\xi=\Lambda(1-m)$, and time $\tau=\Lambda t$, so that Λ drops from the ω equation

$$\omega\partial_\tau\omega = \xi\partial_\xi^2\omega + \partial_\xi\omega - \xi\omega, \tag{8}$$

but enters the integration interval $(0,\Lambda]$, whereas the boundary conditions are $\xi\partial_\xi\omega=0$. The separable solution is $\omega(\xi,\tau)=(\tau_c-\tau)q(\xi)$, while the boundary-value problem for $q(\xi)$ is

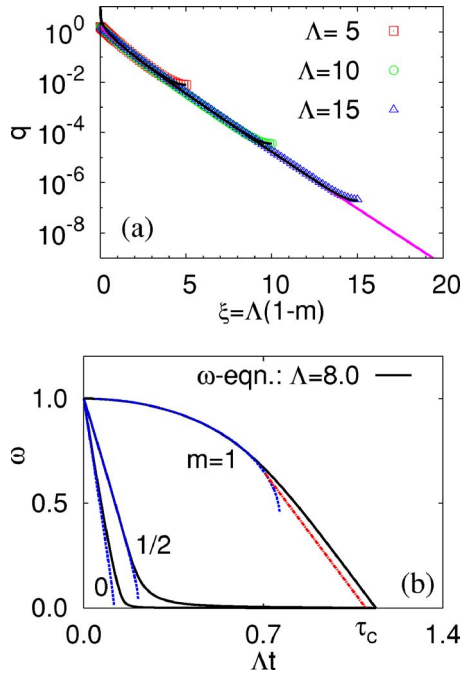

FIG. 4. (Color online) (a) Numerical solutions of Eq. (9) (symbols) and the corresponding "bulk solutions" $q_b(\xi)$ (lines) for $\Lambda=5,10,15$. (b) The implicit solution (10) (the blue lines) versus the numerical solution of the ω-equation (the black lines) for $\Lambda=8.0$ at three Lagrangian points: $m=0,0.5$ and 1.0. The red straight line shows the smoothly matched asymptotic separable solution at $m=1$ (b).

$$(\xi q')' - \xi q + q^2 = 0, \quad \xi q' = 0 \quad \text{at} \quad \xi = 0,\Lambda. \tag{9}$$

At $\xi\gg 1$ $q(\xi)$ is exponentially small, so one can drop the q^2 term and obtain $q_b(\xi)=C[K_0(\xi)+K_1(\Lambda)I_1^{-1}(\Lambda)I_0(\xi)]$ [where $K_{0,1}(\xi)$ and $I_{0,1}(\xi)$ are the modified Bessel functions], which obeys the boundary condition at $\xi=\Lambda$. This solution with $C=0.951$ agrees well with the full numerical solution already at $\xi>1$, see Fig. 4, and therefore is valid everywhere except the thin boundary layer at $m\to 1$. As the q^2 term originates from the $\omega\partial_\tau\omega$ term in Eq. (8), we realize that, almost everywhere, the energy loss at late times is balanced by the heat conduction, while the boundary layer at $m\to 1$ serves as a dynamic "bottleneck" of the cooling.

Outside of a thin boundary layer near $\xi=\Lambda$ (or $m=0$), the solution is close to the solution of the same equation but on the semi-infinite interval $(0,\infty)$. The latter one, $q_\infty(\xi)$, is parameter free and can be found numerically. The shooting starts at the left boundary $\xi=0$ which is a regular singular point of Eq. (9). We demand that $q_\infty''(\xi=0)$ be finite, which yields $q_\infty'(0)=-q_\infty(0)^2$. The shooting procedure gives a unique value of $q_\infty(0)$ for which the solution does not diverge toward $+\infty$ or $-\infty$ at large ξ. We find $q_0\equiv q_\infty(0)=1.633\,356\cdots$; the respective asymptotic profile $q_\infty(\xi)$ is the envelope of the numerical profiles $q(\xi)$ for different Λ in Fig. 4(a).

Early dynamics and collapse time. To find the collapse time t_c [a free parameter in the separable solution (5)], one needs to solve the ω equation with a given initial condition.

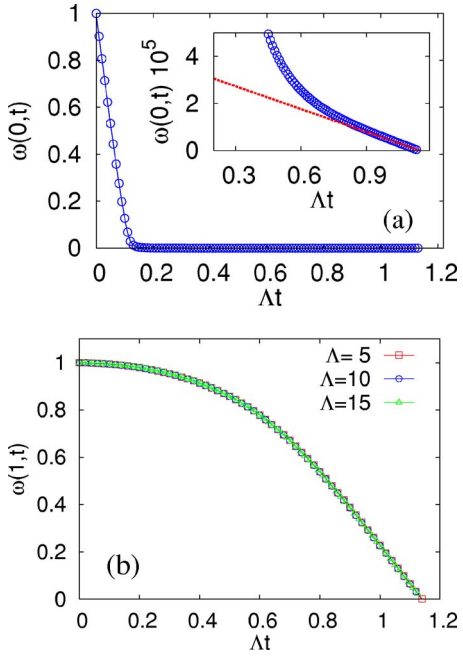

FIG. 5. (Color online) (a) $\omega(m=0,t)$ at $\Lambda=10$. The inset shows a blow-up near τ_c, and the asymptote $(\tau_c-\tau)q(\Lambda)$ (the red dashed line). (b) $\omega(m=1,t)$ vs $\tau=\Lambda t$ for $\Lambda=5,10,15$ collapse into a universal curve.

In general, this can only be done numerically. We obtained analytic estimates of t_c, separately for small and large Λ, for $\omega(m,t=0)=1$.

For $\Lambda \ll 1$ the separable solution (5) and (7) is valid, at order Λ^2, at any $t \geq 0$. This yields the leading-order estimate $t_c \simeq 2\Lambda^{-2}$. For $\Lambda \gg 1$ the initial stage of the cooling dynamics should be addressed separately. We notice that at early times the term $\xi\partial_\xi^2\omega$ in Eq. (8) is small compared to the rest of terms. With this term neglected Eq. (8) reduces to a first-order equation, $\omega\partial_\tau\omega-\partial_\xi\omega=-\xi\omega$, which is soluble by characteristics. The solution $\omega(\xi,\tau)$, in an implicit form, is

$$\sqrt{2}e^{-\xi^2/2}\omega(\xi,\tau)\int_{\xi/\sqrt{2}}^{\sqrt{\xi^2/2-\ln[\omega(\xi,\tau)]}} e^{z^2}dz=\tau, \qquad (10)$$

it is depicted, at points $m=0,1/2$ and 1, in Fig. 4(b). At $\xi \gg 1$ (where most of the gas is located), Eq. (10) predicts an early-time asymptote $\omega(\xi,\tau \ll 1)=1-\xi\tau$ which can be also obtained directly from Eq. (8) with the heat conduction neglected completely. The bottleneck of cooling, however, is at large heights, $\xi \ll 1$, where the gas is very dilute. An early-time asymptote there, as predicted from Eq. (10), is

$$\omega \simeq 1-\xi\tau-\tau^2/2=1-\Lambda^2(1-m)t-\Lambda^2t^2/2. \qquad (11)$$

The implicit solution (10) breaks down, at a given ξ, at time $\tau \sim \min(1,\xi^{-1})$, and then the full ω equation must be solved. Eventually, as τ approaches τ_c, the separable solution (5) emerges.

We stress that, at $\Lambda \gg 1$, the cooling process is highly nonuniform, see Figs. 5(a) and 5(b). For example, at $m=0$ a rapid initial decay $\omega=1-\Lambda^2 t$ crosses over, after a short time

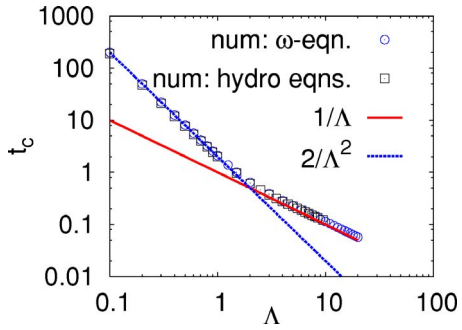

FIG. 6. (Color online) The collapse time vs Λ. Numerical results from the ω equation and from the full hydrodynamic Eqs. (1)–(3) with $\varepsilon=0.025$ are shown by symbols, the small- and large-Λ asymptotes are denoted by lines.

$t \sim \Lambda^{-2}$, into a very slow decay $\omega=\Lambda q(\Lambda)(t_c-t)$, as $q(\Lambda)$ is exponentially small. Meanwhile, at $m=1$ a slow initial decay $\omega=1-\tau^2/2$ crosses over into a rapid decay $\omega=q_0(\tau_c-\tau)$. At $t=t_c$ ω vanishes at *all* ξ (that is, at $y=0$). Note that the dynamics at $m=1$ are independent of Λ in the stretched time $\tau=\Lambda t$.

A good estimate of the collapse time τ_c at large Λ can be obtained by matching, at $\xi=0$, the late-time asymptote $(\tau_c-\tau)q_0$ with the early-time solution (10), see Fig. 4(b). This yields an algebraic equation for τ_c

$$[(\pi/2)^{1/2}\mathrm{erfi}(2^{-1/2}\tau_c^{-1})+q_0^{-1}]=\tau_c\exp[1/(2\tau_c^2)] \qquad (12)$$

which has a unique solution $\tau_c \simeq 1.10$, or $t_c \simeq 1.10\Lambda^{-1}$. For comparison, a numerical solution of Eq. (8), for large Λ, with the initial condition $\omega(\xi,t=0)=1$ yields $\tau_c=1.145$ which agrees with our estimate to about 4%. The slope of the collapsed curves $\omega(\xi=0,\tau)$ for large Λ [Fig. 4(b)] near $\tau=\tau_c$, $\partial_\tau\omega(\xi=0,\tau_c)=1.624$, is in very good agreement with the asymptotic value $q_0=1.633\,356$. Our predictions of the Λ dependence of t_c are summarized in Fig. 6. The small- and large-Λ asymptotes are in excellent agreement with numerical results. Returning to the dimensional units, we observe that, at $\Lambda \ll 1$, the collapse time t_c is much longer than the heat diffusion time. At $\Lambda \gg 1$ t_c is of the order of $(\varepsilon\Lambda)^{-1}t_f \sim (1-r^2)^{-1/2}t_f$ which, for nearly elastic collisions, is much longer than the free fall time t_f.

Having found $\omega(\xi,\tau)$ we can find the rest of hydrodynamic fields. Here we present the results for $\Lambda \gg 1$. In the early stage of cooling the gas density is $n(\xi,\tau)=(\xi/\Lambda)(1-\xi\tau)^{-2}$ and velocity $v(\xi,\tau)=\Lambda(\Lambda-\xi)[(\Lambda+\xi)\tau-2]$. Close to collapse the density $n(\xi,\tau)=\xi(\tau_c-\tau)^{-2}q^{-2}(\xi)$ blows up as $(\tau_c-\tau)^{-2}$. The gas velocity is $v(\xi,\tau)=-2\Lambda(\tau_c-\tau)\int_\xi^\Lambda[q^2(\xi')/\xi']d\xi'$. At $\tau<\tau_c$ it diverges logarithmically at $\xi=0$ (that is, linearly at $y\to\infty$), but vanishes everywhere at $\tau=\tau_c$, while the mass flux nv blows up at $\tau=\tau_c$. Going back to Eulerian coordinate $y=(\tau_c-\tau)^2\int_\xi^\Lambda[q^2(\xi')/\xi']d\xi'$, we see that the velocity field is simply $v(y,t)=-2y/(t_c-t)$.

Summary. Our MD simulations and hydrodynamic theory depict a coherent picture of thermal collapse which develops in the process of a free cooling of a granular gas under gravity. One of the signatures of this picture is the universal

scaling behavior of the total energy $E(t) \sim (t_c - t)^2$ as $t \to t_c$.

It would be interesting to test the quantitative predictions of our theory in experiment. A possible experiment can employ metallic spheres rolling on a slightly inclined smooth surface and driven by a rapidly vibrating bottom wall, as in Ref. [11]. After the "granular gas" reaches a steady state, one stops the driving and follows the cooling dynamics with a fast camera and a particle tracking software. While particle rotation and rolling friction may prove important, we expect that the main predictions of the theory, including the scaling behavior of the total energy at $t \to t_c$, will persist.

L.T. and D.V. are grateful to the U.S. Department of Energy for financial support (Grant No. DE-FG02-04ER46135). B.M. acknowledges support from the Israel Science Foundation (Grant No. 107/05) and from the German-Israel Foundation for Scientific Research and Development (Grant No. I-795-166.10/2003).

[1] P. K. Haff, J. Fluid Mech. **134**, 401 (1983).

[2] J. J. Brey, J. W. Dufty, and A. Santos, J. Stat. Phys. **97**, 281 (1999); I. Goldhirsch, Annu. Rev. Fluid Mech. **35**, 267 (2003); N. V. Brilliantov and T. Pöschel, *Kinetic Theory of Granular Gases* (Oxford University Press, Oxford, 2004), and references therein.

[3] D. C. Rapaport, *The Art of Molecular Dynamics Simulation* (Cambridge University Press, Cambridge, 2004).

[4] In experiment, an (almost) isothermal initial state is easily realized when the particle density N/L_x and the inelasticity $1-r$ are not too large, see, e.g., Ref. [11].

[5] Granular hydrodynamics assumes scale separation, which often demands nearly elastic collisions.

[6] As the gas approaches collapse, a close-packed "condensate" forms, where the dilute gas model breaks down. Therefore, it might seem surprising that it describes the kinetic energy history remarkably well, see Fig. 2(a), until the time of collapse. The reason is that the kinetic energy of the condensate particles is extremely small, and the main contribution to the energy comes from the gas particles.

[7] Y. Bromberg, E. Livne, and B. Meerson, in *Granular Gas Dynamics*, edited by T. Pöschel and N. Brilliantov (Springer, Berlin, 2003), p. 251.

[8] In the expression for the heat flux we omitted a term with the *density* gradient [2]. It can be neglected in the nearly elastic limit.

[9] J. G. Blom and P. A. Zegeling, ACM Trans. Math. Softw. **20**, 194 (1994).

[10] We checked that the ω equation predicts a finite-time collapse for other initial states as well, e.g., when starting from a (nonisothermal) steady state [7], corresponding to a "thermal" bottom.

[11] A. Kudrolli, M. Wolpert, and J. P. Gollub, Phys. Rev. Lett. **78**, 1383 (1997); Phys. Rev. E **67**, 041301 (2003).